ChemComm

COMMUNICATION

View Article Online
View Journal | View Issue

Cite this: *Chem. Commun.*, 2024, **60**, 7902

Received 26th May 2024,
Accepted 4th July 2024

DOI: 10.1039/d4cc02556c

rsc.li/chemcomm

Selective lactic acid synthesis *via* ethylene glycol electrooxidation in borate buffer†

Adarsh Koul, ‡ Shubhadeep Chandra ‡ and Wolfgang Schuhmann *

Efficient and selective oxidation of ethylene glycol is challenging due to uncontrollable C–C bond cleavage. We propose an electrochemical strategy for the selective electrooxidation of ethylene glycol to sythesise lactic acid on a Ni-based electrocatalyst by controlling the pH value of the electrolyte solution.

Lactic acid (LA) has attracted extensive attention owing to its high market demand and its widespread application in food, cosmetics, medicine, textiles, and polymer industries.[1] The current manufacturing method for producing lactic acid relies on biological approaches such as the fermentation of glucose.[2] Moreover, novel chemo-catalytic approaches to produce lactic acid from biomass have also attracted attention in recent years. In this context, Maji and Tu recently developed two alternative approaches for the synthesis of lactic acid based on hydroxide-mediated dehydrogenative crosscoupling between ethylene glycol and methanol.[3,4] However, these biological and chemical approaches suffer from long fabrication periods, poor selectivity as well as reaction conditions such as elevated temperature and pressure, strong alkaline or acidic medium, and tedious workup. Consequently, substantial time and effort have been devoted to finding facile and efficient electrochemical approaches for biomass conversion to valuable chemicals.[5] Electrochemical oxidation of biomass-sourced ethylene glycol is an important topic with its applications not only within the realm of organic synthesis but also as an alternative anode reaction replacing the oxygen evolution reaction (OER) in water electrolysis.[6] A wide range of products, such as glyoxal, glycolaldehyde, glycolic acid, oxalic acid, or their mixtures, have been reported upon ethylene glycol oxidation reaction (EGOR).[7,8] However, it is indeed very challenging to obtain electrooxidised products with high selectivity due to the uncontrollable C–C bond cleavage, while simultaneously achieving high reaction rates and high conversions. Surprisingly, although lactic acid is one of the most high-value-added materials, no reports are on efficient lactic acid production from ethylene glycol electrooxidation. A limited number of studies report highly active EGOR catalysts based on earth-abundant materials and only a few exhibit high selectivity towards value-added products.[9] As for non-noble metal-containing electrocatalysts, Ni-based ones have been the most extensively investigated,[10,11] most in highly basic conditions reporting formic acid as the major product.[10] This suggests that EGOR on Ni-based catalysts involves significant C–C cleavage.[12] Hence, it can be assumed that neutral or slightly less basic electrolytes would circumvent these issues and enable selective EGOR.[13]

We report the first example of selective electrochemical oxidation of ethylene glycol to lactic acid as the major product, using NiOOH as a catalyst and borate buffer as electrolyte. More than 60% selectivity for lactic acid formation was achieved at a current density of 5 mA cm^{-2} at pH 10. It is demonstrated that the selectivity of the EGOR is governed by the electrolyte pH and that the presence of borate buffer solution is more favorable than a highly basic medium for lactic acid formation. Nickel-oxyhydroxide (NiOOH) is a promising anodic material for the EGOR and it is the catalytically active phase during anodic reactions such as OER and EGOR. Considering the activity of NiOOH for the selective electrooxidation of glycerol to 1,3-dihydroxyacetone in buffer solutions as reported previously,[12–14] our initial aim was to investigate the effect of different pH values on the EGOR using NiOOH as active electrocatalyst. Cyclic voltammetry (CV) was first performed in borate buffer solutions using nickel foam (NF) as a working electrode in the absence and presence of ethylene glycol. In the absence of ethylene glycol, the redox feature corresponding to the $Ni^{2+} \rightarrow Ni^{3+}$ transition is visible in the potential range from 1.4 to 1.6 V *vs.* RHE (Fig. 1). At the potential of the initial oxidation of Ni^{2+} a catalytic wave became visible after the addition of EG, in agreement with reports on electrocatalytic oxidation of methanol and ethanol on nickel-based catalysts.[15,16] However, in the presence of ethylene glycol, the $Ni(OH)_2$ oxidation peak was slightly shifted anodically, which could be attributed to an absorption of EG on Ni^{2+} sites making its

Analytical Chemistry – Center for Electrochemical Sciences (CES), Faculty of Chemistry and Biochemistry, Ruhr University Bochum, Universitätsstr. 150, D-44780 Bochum, Germany. E-mail: wolfgang.schuhmann@rub.de

† Electronic supplementary information (ESI) available. See DOI: https://doi.org/10.1039/d4cc02556c

‡ These authors contributed equally to this work.

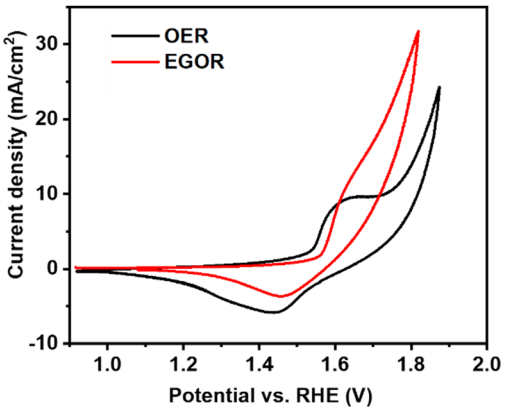

Fig. 1 CV at a Ni foam electrode in the absence and presence of 0.1 M ethylene glycol in borate buffer solution at pH 10 at a scan rate of 10 mV s^{-1}.

oxidation more difficult (Fig. S2, ESI†).[17] The impact of borate buffer solutions with different pH values on the product distribution was investigated by chronopotentiometry using an electrochemical flow-through electrolyser with the anode and cathode compartments being separated by an anion-exchange membrane (Fig. S1, ESI†).

Specifically, different buffer solutions with pH values from 7–13 in the absence and presence of 1 M ethylene glycol were pumped from their respective reservoirs to the anode and cathode compartments, respectively, and recirculated throughout the entire duration of the measurement while a constant current density of 5 mA cm^{-2} was applied. At certain time intervals, samples of the electrolyte were collected from the anode compartment and diluted for subsequent HPLC analysis to monitor the formed EGOR products. The corresponding product selectivity of the major and minor products formed after passing the same amount of charge after one hour for each condition is shown in Fig. 2.

Formic acid (FA) was obtained as the major product in 1 M KOH, which indicates significant C–C bond cleavage in a highly basic medium.[10] The only other detectable product was glycolic acid (GCA) and no lactic acid (LA) was detected in 1 M KOH. Surprisingly, when the reaction was carried out in borate buffer, a remarkable change in product selectivity was observed. At pH 7, the formation of formic acid was significantly diminished, and LA was obtained as the major product, suggesting that C–C bond cleavage is less favored in borate buffer at pH 7 (Fig. 2).[12,13] The selectivity of LA reached 60% and that of FA decreased from 80 to 30% compared to that in 1 M KOH. This could be attributed to the formation of borate–ethylene glycol coordination complexes such as didiolborates which prevent primary oxidation products such as glycolaldehyde from being further oxidized to FA.

The selectivity of LA remained nearly the same over the range of pH from 7 to 10. However, upon further increasing the pH of the solution from 10 to 12 the selectivity of LA decreased from 60 to 30% and the other oxidation products such as FA and GLA showed an increasing trend in their selectivity. A similar selectivity trend was also observed after 3 h of

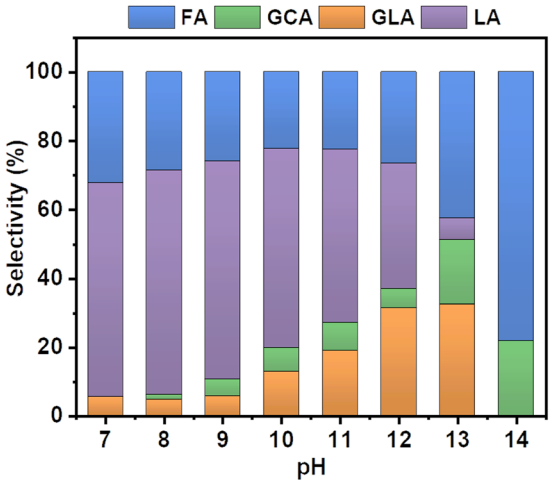

Fig. 2 Product selectivity of the EGOR after one hour of electrolysis at a constant current density of 5 mA cm^{-2} at various pH conditions. Formic acid (FA), lactic acid (LA), glycolic acid (GCA), and glyceric acid (GLA).

electrolysis (Fig. S3, ESI†). The sum of faradaic efficiencies for all detected products is shown in Fig. 3. When EGOR was performed at pH 7 in borate buffer, the FE% of LA reached 20%. However, the total FE decreased significantly in borate buffer at pH 7 compared to that in 1 M KOH, indicating that the alkaline medium facilitates the EGOR. The higher activity of alcohol oxidation in alkaline medium is probably due to the base-catalyzed deprotonation of the alcohol groups, which results in the formation of more reactive alkoxide species. Given the higher activity of EGOR in alkaline medium and the promising trend of increased LA selectivity with increasing solution pH, we further increased the solution pH to 10. The FE of LA as well as total FE increased and reached a maximum value (Fig. 3). The concentration profile showed a similar trend with higher concentrations obtained at pH 10 (Fig. S4, ESI†). For the EGOR in 1.0 M borate buffer solution at pH 10, Ni foam

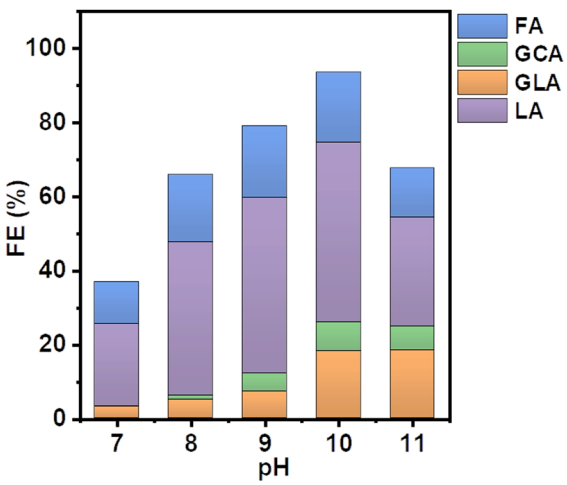

Fig. 3 Faraday efficiencies (FE) of the EGOR at a constant current density of 5 mA cm^{-2} at various pH conditions in the presence of borate.

exhibits a potential of 1.85 V *vs.* RHE at a current density of 5 mA cm^{-2} and yields LA as the major product (Fig. S5, ESI†).

The significantly enhanced FE at higher pH is probably due to the formation of negatively charged borate–ethylene glycol complexes, which can migrate to the positively charged anode and by this facilitate the oxidation reaction.[14] Therefore, the coordination effect of the borate ion with ethylene glycol not only enhances the electrochemical activity of ethylene glycol but also prevents the intermediate products from being further oxidized, resulting in high selectivity and FE of LA at pH 10 among the collected liquid products (60% selectivity and FE of 50%).

Separate from pH, the applied current density is also a key factor that affects the product selectivity and concentration of the products formed during EGOR. Therefore, EGOR activity was further explored by changing the current density from 5 to 20 mA cm^{-2} (Fig. S5, ESI†). The concentration of the formed LA increased from nearly 8 mM to 20 mM with the increase of current density from 5 to 20 mA cm^{-2}. However, the selectivity of LA slightly decreased from a current density of 5 mA cm^{-2} to 20 mA cm^{-2}, accompanied by an increase in the selectivity of FA (Fig. 4). High activity of NiOOH at high current density and concomitantly increased applied potential enhances the C–C bond cleavage resulting in a low selectivity for LA.

To further investigate the mechanism of EGOR over Ni foam, potential-dependent *in situ* Raman spectra were collected in the presence and absence of ethylene glycol in borate buffer (Fig. 5).

In the absence of ethylene glycol and at potentials higher than 1.5 V *vs.* RHE, two bands appear at 491 and 568 cm^{-1} corresponding to the Ni–O vibrations in NiOOH. The intensity of the NiOOH bands increases with increasing potentials. However, in the presence of ethylene glycol, the NiOOH band does not appear until the potential reaches 1.7 V *vs.* RHE, and then the intensity of the Ni–O bands at 500 and 577 cm^{-1} increases gradually with increasing potential. The blue shift in the NiOOH bands could be attributed to positive charge storage on the catalyst surface upon EGOR.[18] Based on this

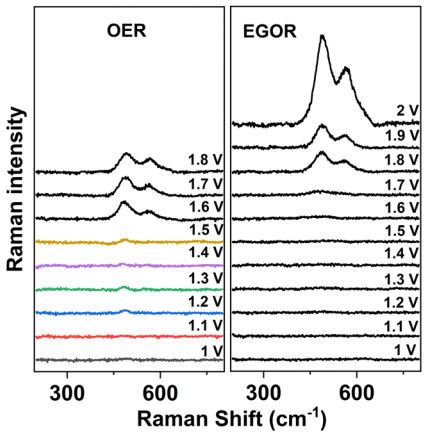

Fig. 5 Potential-dependent Raman spectra of a Ni foam anode in the absence of ethylene glycol (left, OER) and in the presence of ethylene glycol (EGOR, right).

experimental evidence, it is suggested that similar to the OER, Ni^{2+} is first oxidized to NiOOH, and then ethylene glycol can be oxidized by NiOOH accompanied by the corresponding transformation from NiOOH back into Ni^{2+}, so that the NiOOH band in the *in situ* Raman spectra cannot be detected at the beginning of EGOR.[16]

A plausible mechanism for the electrochemical oxidation of ethylene glycol to LA is depicted in Scheme 1. Ethylene glycol is first oxidized by NiOOH to glycolaldehyde irrespective of the pH value of the electrolyte. Both hydroxyl and aldehyde groups in glycolaldehyde are reactive at the anode; however, their reactivities are strongly dependent on the pH value of the electrolyte solution. In an alkaline medium, the aldehyde group is easily oxidized to the acid group resulting in the formation of GCA.[13] Therefore, GCA and FA were obtained as the main products in 1 M KOH. However, in borate buffer, an opposite trend is observed. Glycolaldehyde mainly undergoes cross-aldol condensation with the formed formaldehyde to generate glyceraldehyde. It is known that during electrooxidation of *e.g.* glycerol formate is formed after C–C bond cleavage. In these cases and the absence of the borate buffer the initially obtained formaldehyde is immediately further oxidized. In the presence of

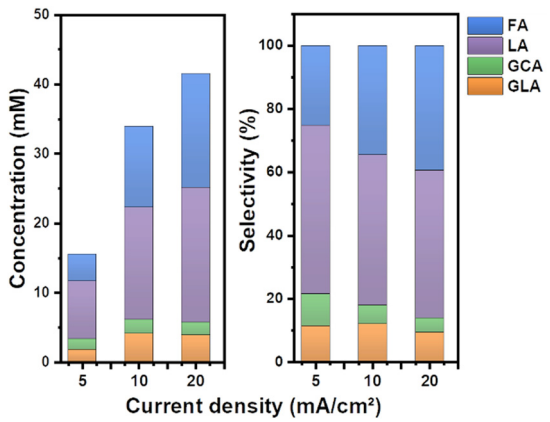

Fig. 4 (a) Product distributions showing concentrations at different current densities. (b) Product selectivity of the EGOR at different current densities in a borate buffer solution at pH 10.

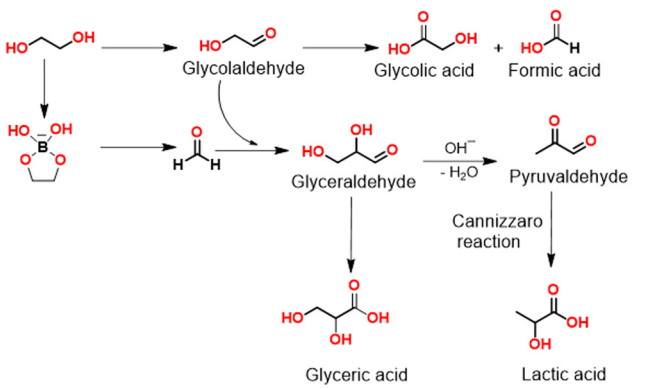

Scheme 1 Suggested mechanism for the electrochemical oxidation of ethylene glycol in borate buffer.

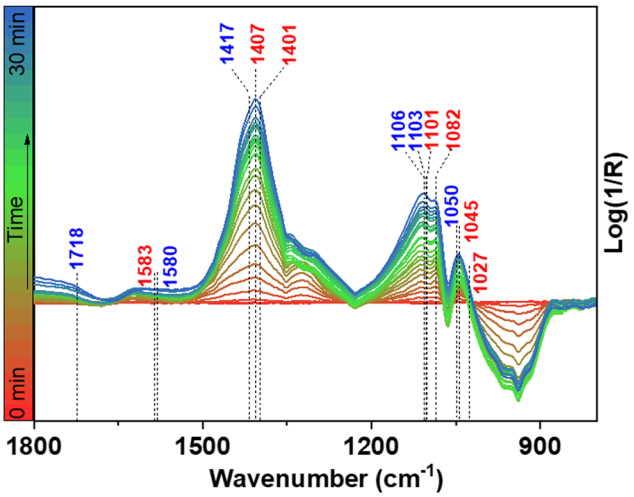

Fig. 6 FTIR spectra recorded during EGOR on Ni foam in a borate buffer at pH 10.

borate buffer, a didiolborate is formed between borate and ethylene glycol and we suppose that this will be the species which interacts with the catalyst surface. Oxidative C–C-bond cleavage would then form a protected formaldehyde which may escape from the catalyst surface and is available for the follow-up aldol condensation with glycolaldehyde.

Alternatively, it cannot be excluded that lactic acid is formed through glyceric acid dehydroxylation. However, dehydroxylation of glyceric acid would initially lead to the formation of pyruvic acid, and further conversion of pyruvic acid to lactic acid is a reduction reaction which may be unlikely in oxidative alkaline conditions. Since glycolaldehyde and glyceraldehyde can be easily converted to GCA, GLA, and LA in borate buffer, it is difficult to detect them by HPLC. Therefore, to further evaluate the reaction mechanism and the involved intermediates during the LA formation, *in situ* Fourier-transformed infrared spectroscopy (FTIR) was carried out using a NF electrode integrated into a borehole electrode in borate buffer at pH 10 (Fig. S6, ESI†).[19] As shown in Fig. 6, the *in situ* FTIR spectra show typical band ν(C–O) of glycolaldehyde at 1050 and 1082 cm^{-1} (Fig. S7, ESI†).[8] Further conversion of glycolaldehyde to glyceraldehyde can be confirmed by the appearance of a new band at 1045 cm^{-1}, together with the band of LA (1103 cm^{-1}) (Fig. S8, ESI†). In addition, the formation of other carboxyl compounds is also confirmed by FTIR bands such as GCA (1407 cm^{-1}), and GLA (1583 cm^{-1}), (Fig. S7 and S8, ESI†) in agreement with the HPLC results. For conversion of glyceraldehyde to LA, glyceraldehyde undergoes a base dehydration to form pyruvaldehyde which is then converted to LA by means of an intramolecular Cannizzaro reaction under basic conditions.[3,4]

In summary, we have demonstrated for the first time selective electrooxidation of ethylene glycol to LA over a NiOOH catalyst with more than 60% selectivity in a borate buffer solution. Our results provide new insights into the selective conversion of biomass-derived polyols to value-added products on non-noble metals-based catalysts.

The authors are grateful for the financial support from the Deutsche Forschungsgemeinschaft (DFG) in the framework of the research unit FOR 2982 "UNODE" ([413163866]) and the CRC247 [388390466].

Data availability

Data for this article are available at Zenodo at **https://doi.org/10.5281/zenodo.12529990**.

Conflicts of interest

There are no conflicts to declare.

Notes and references

1 (*a*) M. S. Holm, S. Saravanamurugan and E. Taarning, *Science*, 2010, **328**, 602–605; (*b*) M. Dusselier, P. van Wouwe, A. Dewaele, E. Makshina and B. F. Sels, *Energy Environ. Sci.*, 2013, **6**, 1415–1442.
2 (*a*) L. S. Sharninghausen, J. Campos, M. G. Manas and R. H. Crabtree, *Nat. Commun.*, 2014, **5**, 5084; (*b*) Y. Zhu, C. Romain and C. K. Williams, *Nature*, 2016, **540**, 354–362.
3 J. Wu, L. Shen, Z.-N. Chen, Q. Zheng, X. Xu and T. Tu, *Angew. Chem., Int. Ed.*, 2020, **59**, 10421–10425.
4 S. Waiba, K. Maji, M. Maiti and B. Maji, *Angew. Chem., Int. Ed.*, 2023, **62**, e202218329.
5 A. C. Brix, D. M. Morales, M. Braun, D. Jambrec, J. R. C. Junqueira, S. Cychy, S. Seisel, J. Masa, M. Muhler, C. Andronescu and W. Schuhmann, *ChemElectroChem*, 2021, **8**, 2336–2342.
6 C. Jin, Y. Song and Z. Chen, *Electrochim. Acta*, 2009, **54**, 4136–4140.
7 (*a*) D. Si, B. Xiong, L. Chen and J. Shi, *Chem. Catal.*, 2021, **1**, 941–955; (*b*) N. L. Chauhan, V. A. Juvekar and A. Sarkar, *Electrochem. Sci. Adv.*, 2022, **2**, e2100092.
8 Y. Yan, H. Zhou, S.-M. Xu, J. Yang, P. Hao, X. Cai, Y. Ren, M. Xu, X. Kong, M. Shao, Z. Li and H. Duan, *J. Am. Chem. Soc.*, 2023, **145**, 6144–6155.
9 D. M. Morales, D. Jambrec, M. A. Kazakova, M. Braun, N. Sikdar, A. Koul, A. C. Brix, S. Seisel, C. Andronescu and W. Schuhmann, *ACS Catal.*, 2022, **12**, 982–992.
10 J. Li, L. Li, X. Ma, X. Han, C. Xing, X. Qi, R. He, J. Arbiol, H. Pan, J. Zhao, J. Deng, Y. Zhang, Y. Yang and A. Cabot, *Adv. Sci.*, 2023, **10**, e2300841.
11 R. Samanta, A. Shekhawat, P. Sahu and S. Barman, *Energy Fuels*, 2024, **38**, 73–104.
12 M. K. Goetz, M. T. Bender and K.-S. Choi, *Nat. Commun.*, 2022, **13**, 5848.
13 R. Ge, Y. Wang, Z. Li, M. Xu, S.-M. Xu, H. Zhou, K. Ji, F. Chen, J. Zhou and H. Duan, *Angew. Chem., Int. Ed.*, 2022, **61**, e202200211.
14 X. Huang, Y. Zou and J. Jiang, *ACS Sustainable Chem. Eng.*, 2021, **9**, 14470–14479.
15 M. T. Bender, R. E. Warburton, S. Hammes-Schiffer and K.-S. Choi, *ACS Catal.*, 2021, **11**, 15110–15124.
16 Y. Yan, J. Zhong, R. Wang, S. Yan and Z. Zou, *J. Am. Chem. Soc.*, 2024, **146**, 4814–4821.
17 M. T. Bender and K.-S. Choi, *ChemSusChem*, 2022, **15**, e202200675.
18 D. Chen, X. Xiong, B. Zhao, M. A. Mahmoud, M. A. El-Sayed and M. Liu, *Adv. Sci.*, 2016, **3**, 1500433.
19 S. Cychy, D. Hiltrop, C. Andronescu, M. Muhler and W. Schuhmann, *Anal. Chem.*, 2019, **91**, 14323–14331.